Improving the efficiency of electric machines using ferrofluids

2006 J. Phys.: Condens. Matter 18 S2985

(http://iopscience.iop.org/0953-8984/18/38/S31)

INSTITUTE OF PHYSICS PUBLISHING JOURNAL OF PHYSICS: CONDENSED MATTER

J. Phys.: Condens. Matter **18** (2006) S2985–S2998 doi:10.1088/0953-8984/18/38/S31

Improving the efficiency of electric machines using ferrofluids

A Nethe, Th Scholz and H-D Stahlmann

Brandenburg University of Technology, Chair of Electromagnetic Theory and Process Modelling, PO Box 101344, 03013 Cottbus, Germany

E-mail: Thomas.Scholz@tet.tu-cottbus.de

Received 2 May 2006, in final form 15 July 2006
Published 8 September 2006
Online at stacks.iop.org/JPhysCM/18/S2985

Abstract

Ferrofluids have a growing importance in technical and medical applications since stable suspensions of magnetic nanoparticles in carrier fluids can be produced. The application of these strong paramagnetic fluids in electric machines by filling the air-gap between stator and rotor to increase the force in linear and the momentum in rotating machines offers an interesting possibility to improve efficiency and thus to save energy. Some calculations of this effect are presented here, including the method of magnetic circuits and field theory. Also, peripheral aspects such as fluid friction and thermal implications are discussed. Experimental verification by testing linear and rotating machines will confirm the positive results.

(Some figures in this article are in colour only in the electronic version)

1. Introduction

Magnetic fluids, which are a suspension of magnetic nanoparticles in a carrier fluid, covered with a tensid layer to prevent clustering, have super-paramagnetic properties. This high permeability can be used in several applications, since the improvement in chemical technology during the last years provides fluids with high saturation magnetization, relatively low viscosity and above all long-term stability. One option of technical application, which is treated in this paper, is the amplification of force or torque in linear or rotating electric machines by filling the fluid in the gap between stator and rotor. Thus the magnetic resistance of the air-gap is reduced.

A remarkable force amplification in linear or rotating electric machines is predicted on account of theoretical investigations. These calculations, beginning with a rough estimation using the method of magnetic circuits and followed by a more precise evaluation with field calculations, are presented here. The theoretical investigations are completed with peripheral aspects such as additional friction due to the influence of the liquid between mutually moved magnets and thermal implications which concern the thermal flow through the gap between

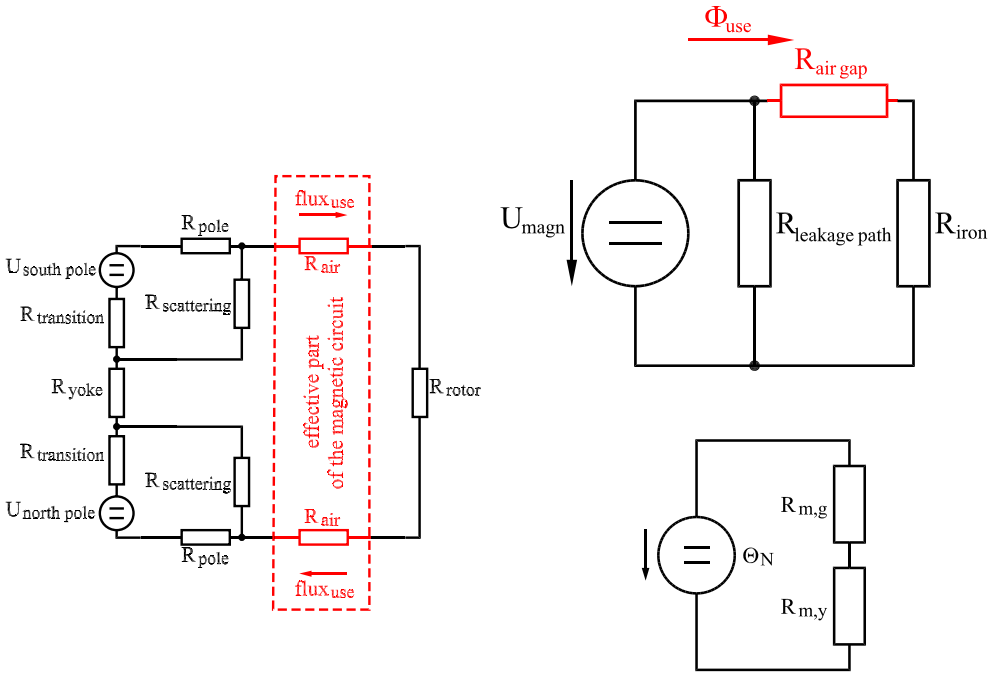

Figure 1. Magnetic circuit of an DC electric machine (left) and its simplification with leakage flux (right, top) and without leakage flux (right, bottom).

the magnets where air is exchanged by a ferrofluid. The very promising theoretical results for both the linear and the rotating machines have to be proved by experiments. This is done with a linear and a rotating electric machine. Beyond the pure amplification effect a lot of effects are involved in running a real motor. Therefore it is necessary to point out the limits and the technological difficulties of this invention.

2. Theoretical evaluation of the ponderomotive interaction enforced by ferrofluids

2.1. Magnetic circuits

Magnetic systems with small losses (closed lines of flux) can be described with magnetic circuits analogous to electric circuits. The circuit representing an electric motor is shown in figure 1.

With the quantities

U_N	magnetic voltage	I	electric current
N	number of current bends	R_m	magnetic resistance
$G_\mathrm{m} = 1/R_\mathrm{m}$	magnetic conductivity	A	area (air-gap, yoke)
l	length (air-gap, yoke)	Φ_m	magnetic flux
B	flux density	μ_r	relative permeability

and applying simple circuit design the effect of ferrofluids in the gap is evaluated by the formula

$$B = U_N \mu_0 \frac{\mu_{\mathrm{r},g}\mu_{\mathrm{r},y}}{l_g \mu_{\mathrm{r},y} + l_y \mu_{\mathrm{r},g}} = U_N \mu_0 G_\mathrm{m}. \tag{1}$$

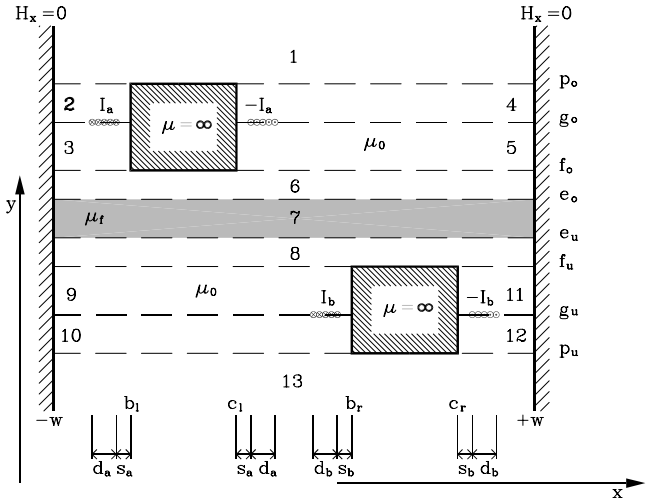

Figure 2. Geometry of the linear electric machine model.

To compare the magnetic circuit with and without ferrofluid three different cases are mentioned. The used permeabilities are typical numbers for the materials. They can be taken from tables [1]. The lengths follow common small electric machines for all three cases: $l_g = 1$ mm, $l_y = 30$ mm.

- Gap is filled with air: $\mu_{\mathrm{r},g} = 1$, $\mu_{\mathrm{r},y} = 20\,000 \Rightarrow \boxed{G_\mathrm{m} = 998\ \mathrm{V\ s\ A^{-1}}}$.
- Gap is filled with ferrofluid, μ of the yoke remains unchanged (iron unsaturated): $\mu_{\mathrm{r},g} = 2$, $\mu_{\mathrm{r},y} = 20\,000 \Rightarrow \boxed{G_\mathrm{m} = 1994\ \mathrm{V\ s\ A^{-1}}}$.
- Gap is filled with ferrofluid, μ of the yoke sinks with increased field strength (iron saturated): $\mu_{\mathrm{r},g} = 2$, $\mu_{\mathrm{r},y} = 1000 \Rightarrow \boxed{G_\mathrm{m} = 1887\ \mathrm{V\ s\ A^{-1}}}$.

A doubling of the gap permeability delivers nearly a doubling of the whole conductivity in the second case. Taking the nonlinearity into account reduces this effect slightly, but a significant gain remains.

2.2. Magnetic forces calculated by field theory

The method used here is orthogonal expansion of Fourier series, which represent the field strength. The coefficients of these series are found by matching the boundary conditions of field strengths between the rectangular or rotational symmetric subspaces, into which the whole area of investigation is divided. A more detailed explanation of the method of orthogonal expansion is given in [2].

2.2.1. Linear electric machines. Figure 2 shows the configuration of the treated model including the arrangement of the subspaces. The objects indicated with $\mu = \infty$ represent the two magnets acting on each other and which are moved horizontally in an actual electric machine. In the gap between the two magnets three subspaces (6, 7, 8) are chosen to make it possible to simulate a partially filled gap. The magnet coils are realized by the current sheets ($\pm I_a$, $\pm I_b$) between two subspaces respectively (2–3, 4–5, 9–10, 11–12).

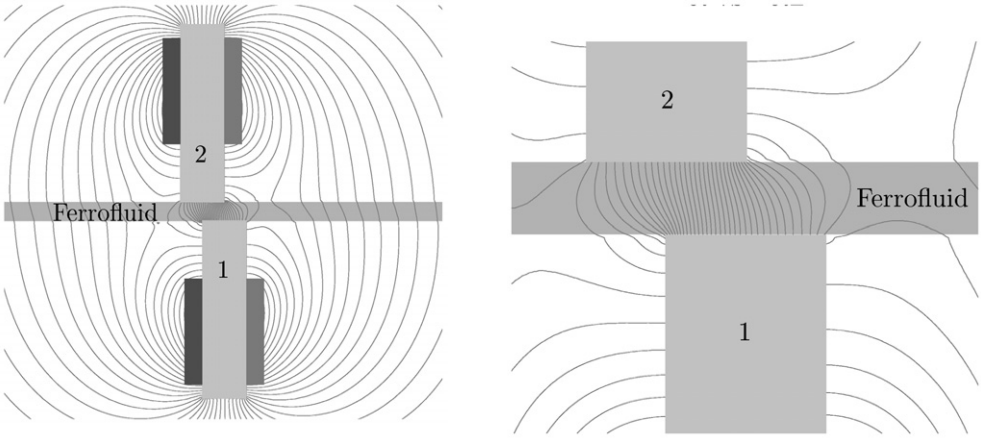

Figure 3. Lines of force for the linear motor (1, lower magnet; 2, upper magnet); the whole structure left, the gap area right.

As an example of the mathematical ansatz the vector potential of subspace 3 is mentioned:

$$A_{z,3}(x, y) = \sum_{j=1}^{n_3} \cos(k_{3,j}[x - b_l])(\exp(k_{3,j}[y - g_o])A_{3,j} + \exp(-k_{3,j}[y - f_o])B_{3,j}). \tag{2}$$

The number of addends n_3 determines the precision of the result. The eigenvalues $k_{3,j}$ are found using the boundary conditions at the vertical walls. These walls, which do not exist in reality, are necessary for obtaining finite series. Placing them at a sufficient distance, their influence on the resulting forces between the two magnets is negligible. With the continuation requirements of the tangential magnetic field strength and the vertical magnetic flux between two subspaces respectively the coefficients are found via a system of linear equations.

The forces between the two magnets are calculated by application of the Maxwell stress tensors [7]. They will be integrated along the limits of one magnet:

$$\oint_{\text{contour enclosing the magnet}} (\mathbf{Bn})\mathbf{H} - 0.5(\mathbf{BH})\mathbf{n}\,\mathrm{d}S \tag{3}$$

with the magnetic flux **B**, the magnetic field strength **H** and the normal vector **n**.

Figure 3 shows the lines of force for the configuration treated here: the whole area on the left, as a detail the gap on the right. In figure 4 the absolute value of the horizontal force versus the relative permeability in the gap for some widths of the gap is depicted. The wider the gap is, the more significant is the amplification effect. This result is as expected. It is remarkable that for a permeability value of about 4–5 the force reaches a maximum and drops for greater permeabilities. This maximum value is beyond the ferrofluids available today, but for the future this effect has to be kept in mind.

2.2.2. Rotating electric machines. Figure 5 (left) shows the geometry of the radial layer model. The gap area is subdivided into several subspaces. In each one a different relative permeability is used, which is determined during the calculation in a recursive process as well as the variable permeability in the stator and rotor. Recursive means that the first time the field strengths are determined with a start value of permeability. Then applying these fields new

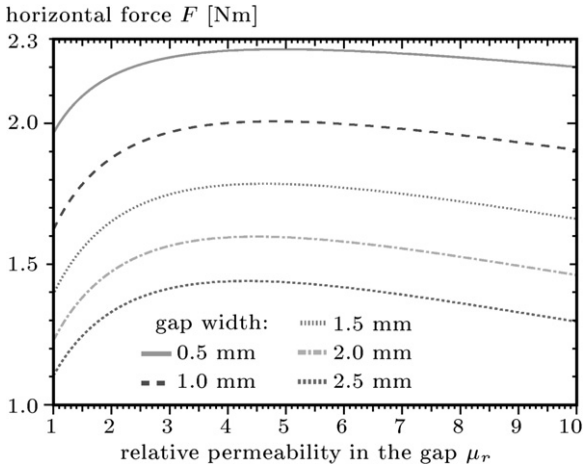

Figure 4. Horizontal force versus the relative permeability μ_r for some gap widths.

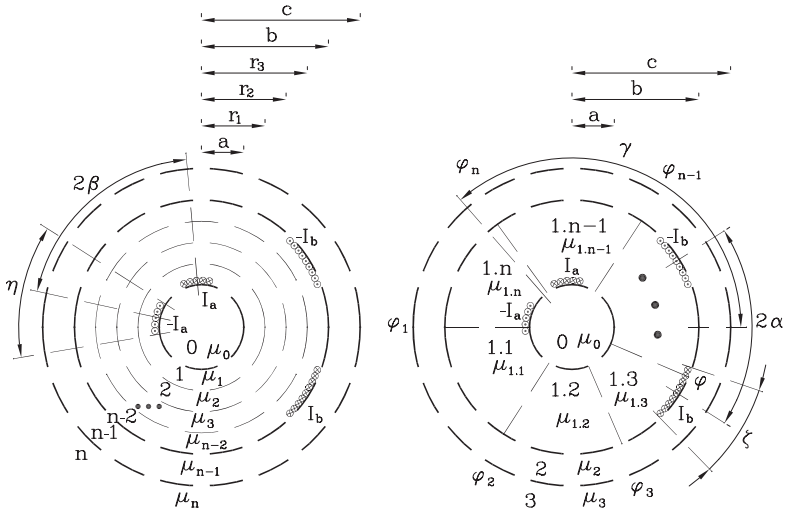

Figure 5. Geometry of the n-layer model of a rotating electric machine, with radial layers (left) and azimuthal sections (right) in the gap between stator and rotor.

permeabilities are gained for a rerun of the calculation. This is done until the difference of field values between two runs of calculation falls below a preselected value.

Cylindrical coordinates are used. In each rotational symmetric subspace an ansatz of the following type is made for the field excited by the stator current:

$$
\begin{aligned}
A_{z,i}(\varrho,\varphi) &= \sum_{j=1}^{n}\left(\frac{\varrho}{r_i}A_{j;i}+\frac{r_i}{\varrho}B_{j;i}\right)\sin(j\varphi),\\
H_{\varphi,i}(\varrho,\varphi) &= \frac{1}{\mu_i}\sum_{j=1}^{n}\frac{j}{\varrho}\left(\frac{\varrho}{r_i}A_{j;i}-\frac{r_i}{\varrho}B_{j;i}\right)\sin(j\varphi),\\
B_{\varrho,i}(\varrho,\varphi) &= \sum_{j=1}^{n}\frac{j}{\varrho}\left(\frac{\varrho}{r_i}A_{j;i}+\frac{r_i}{\varrho}B_{j;i}\right)\cos(j\varphi).
\end{aligned}
\tag{4}
$$

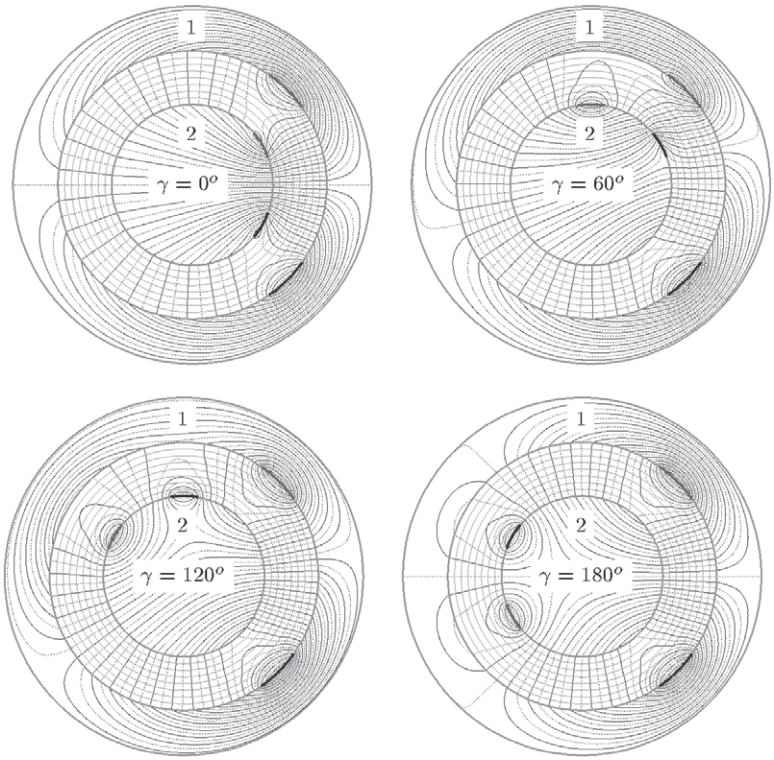

Figure 6. Magnetic lines of force for the n-layer model (eight layers in the gap between stator and rotor) for four different angles γ between the currents (1, stator; 2, rotor).

ϱ is the radius coordinate. The following boundary conditions have to be fulfilled:

$$\begin{aligned} &H_{\varphi,i+1}(\varrho = a; r_i; b, \varphi) - H_{\varphi,i}(\varrho = a; r_i; b, \varphi) = 0;\ J_a(\varphi);\ J_b(\varphi), \\ &B_{\varrho,i+1}(\varrho = a; r_i; b, \varphi) - B_{\varrho,i}(\varrho = a; r_i; b, \varphi) = 0. \end{aligned} \tag{5}$$

Solving the resulting linear system of equations determines the coefficients $A_{j;i}$, $B_{j;i}$ and thus gives the fields, from which the torque is obtained by the Maxwell stress tensor. A comprehensive presentation of this derivation can be found in [3]. The concept of the stress tensor is explained in detail in [7].

Figure 5 (right) shows the azimuthal segment model. Here the first step is finding the eigenvalues in the subdivided gap subspaces. Then the whole field, and from it the torque, is calculated as before.

As an example of a field configuration in a rotating electric machine, figure 6 shows the lines of force for the radial layer model applied to four different angle values between the currents. The gap is made excessively wide to better recognize the field configuration.

The left graph in figure 7 shows the relative torque using the calculation with radial layers for several types of ferrofluid with different saturation magnetizations related to the case with an air filled gap versus the gap width; in the right graph the same is depicted for the calculation with azimuthal segments. Compared to the left graph the azimuthal segmented model delivers a lower increase of torque. This happens due to the fact that the variation of field strength varies more in the azimuthal direction than in the radial one, thus the nonlinearity of the magnetic

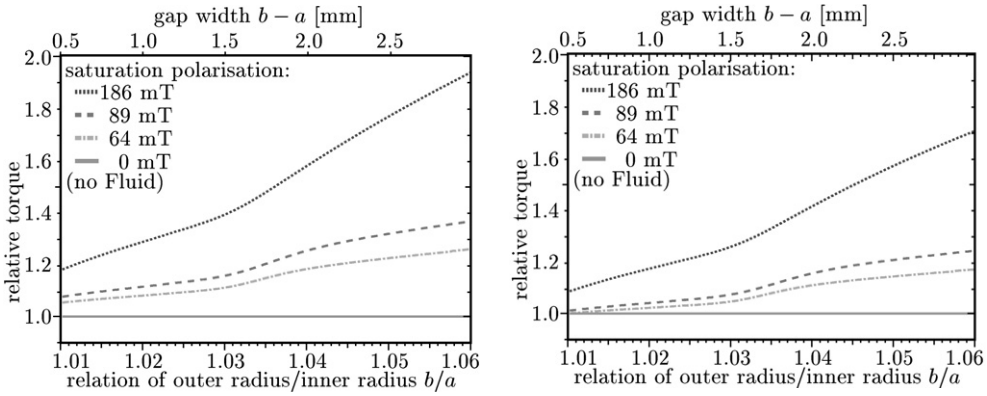

Figure 7. Relative torque versus the gap width for three ferrofluids, to the left calculated with the radial layer, to the right with the azimuthal segment model.

fluid material appears more intense. The order of magnitude corresponds to the result obtained with the rectangular configuration.

Comparing figure 4 with 7 one sees that the gain of torque or force in the case of a rotating machine is greater than in the case of a linear machine. As a reason the magnetically more closed structure in the model of the rotating machine is a possibility. Thus in the linear model the scattering losses are more substantial and related to this phenomenon the influence of the ferrofluid is less remarkable. Constructing a machine design suited for operation with ferrofluids, this point has to be taken into account.

2.3. Calculation of friction losses

The opposing momentum caused by fluid friction excited by a fluid between two coaxial mutually rotating cylinders is calculated due to the Couette flow [6]:

$$\sigma_{\varphi\varrho} = \eta\varrho\frac{\partial}{\partial\varrho}\left(\frac{v_\varphi}{\varrho}\right) = -\frac{2B\eta}{\varrho^2}, \qquad B = \frac{(\omega_1-\omega_2)b^2a^2}{b^2-a^2}, \tag{6}$$

with η the viscosity, ω the angular frequency, a and b the radii of the inner and outer cylinder and ϱ the radius coordinate in cylindrical coordinates.

The viscosity of a fluid depends on temperature, on concentration of particles in a colloid, which is the most important term for ferrofluids, and on the strength of the magnetic field for a paramagnetic fluid.

Figure 8 shows the opposing momentum per length versus the rotational speed for several gap widths. The round dots limit the validity of the given Couette-flow formula. To the right of these dots Taylor–Couette instabilities occur. For the viscosity a value of $\eta = 59$ mPa s is used, which is an average value of commercial ferrofluids. For a higher magnetization and thus viscosity the momentum grows.

Comparing the opposing moments with those resulting from the reduced magnetic resistance due to the ferrofluids, the maximum rotational speed with a remaining positive torque gain is about 2000–3000 rpm.

2.4. Estimation of thermal behaviour in an electric machine

Due to Joule heat an electric machine has to be cooled. The ferrofluid can be a great help to do it by conducting the heat of the rotor better than the air filled gap.

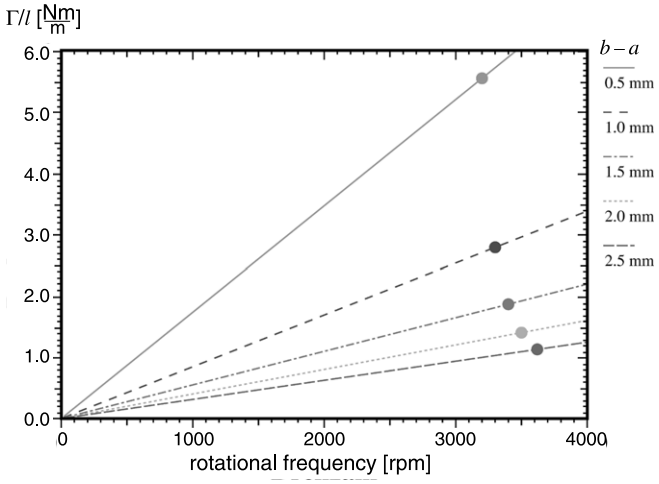

Figure 8. Opposing momentum per length caused by fluid friction versus the rotational speed for several gap widths; $\eta = 59$ mPa s, $b = 30$ mm; to the right of the round dots the solution loses validity due to vortices (Taylor instability).

The stationary heat transfer in cylindrical coordinates is described by the following differential equation:

$$\dot{Q} = -\lambda A \frac{\mathrm{d}\vartheta}{\mathrm{d}r}. \tag{7}$$

with the temperature ϑ, the transfer coefficient λ and the surface A. For a coaxial multilayer system one gets the well known formula for the heat flux:

$$\dot{Q} = \frac{2\pi L(\vartheta_1 - \vartheta_{n+1})}{\frac{1}{\lambda_1}\ln\frac{r_2}{r_1} + \frac{1}{\lambda_2}\ln\frac{r_3}{r_2} + \frac{1}{\lambda_3}\ln\frac{r_4}{r_3} + \cdots + \frac{1}{\lambda_n}\ln\frac{r_{n+1}}{r_n}} \tag{8}$$

with $r_1, r_2, \ldots, r_n$ the radii of the different layers and L the length of the cylinder.

In figure 9 is given a comparison between the supplementary amount of heat flux which occurs with feeding the gap between rotor and stator with a ferrofluid and the additional heat created by the fluid friction. The first one is depicted with solid lines for several specific heat conductance coefficients indicated with an arrow in the direction of growing values, which are representative for ferrofluids. The contribution of friction heat is presented for three rotational speeds with the dotted lines. The difference between a solid and a dotted line is the net amount of heat flux gain, positive or negative. One sees that over a wide parameter range a positive gain of heat flux is possible. This means that the electric energy fed to the machines can be raised or the construction of the whole motor can be designed to be more compact.

3. Experimental verification of the ponderomotive interaction enforced by ferrofluids

3.1. Linear electric machines

The motivation of applying this model of a linear electric machine is to eliminate the friction and thus to measure the pure force amplification. A second point is the aimed application on pulse motors, which is simulated here with a toothed magnet surface.

In figure 10 the principle of measurement for flat magnet surfaces can be seen, representing a continuous electric drive (left), and for grooved magnet surfaces, simulating a stepping motor

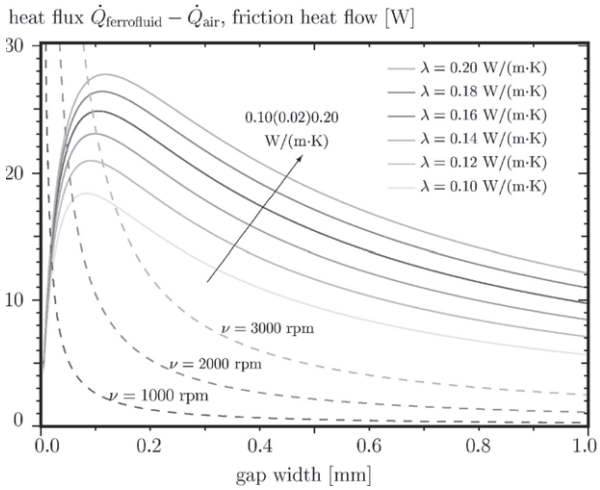

Figure 9. Heat flux versus the gap width between stator and rotor. The solid lines represent the gain of heat dissipation for typical values of thermal conductivity for several ferrofluids in the gap area, the dotted lines the additional heat created by the fluid friction; the arrow indicates the growth of the parameter.

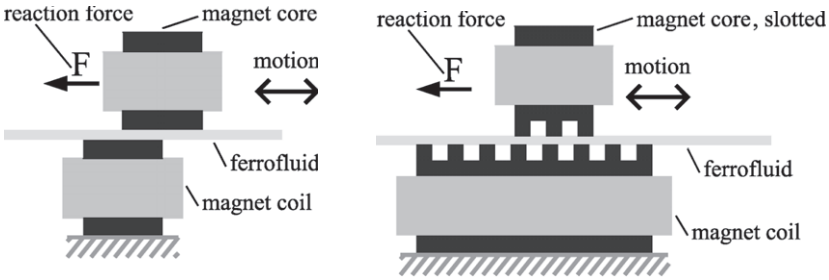

Figure 10. Principle of measurement for a simple linear machine (left) and for a stepping motor (right).

(right). The two magnets are moved mutually. The reaction forces (lateral forces) of the two horizontal moved electromagnets are measured.

Figure 11 shows a photograph of the linear electric machine, where the major parts can be recognized. The lower electromagnet is fixed. The upper moves on ball bearings on polished steel round rods. This reduces the force due to rolling friction down to a maximum of 0.03 N. The distance between the magnets is controlled by a caliper with micrometer resolution. The upper magnet can be exchanged (flat surface, toothed surface). A trough is filled with the fluid. In its bottom the lower magnet is built in. The forces are measured with a DMS based force sensor by a computer aided measuring system. This DMS based force sensor can be seen in the background.

The following demands are fulfilled by the measurement set-up:

- the forces, which are acting between the lateral moved electromagnets, can be measured;
- precise adjustment of the gap width between the two magnetic poles;
- balancing out of the whole apparatus to avoid effects of gravity;

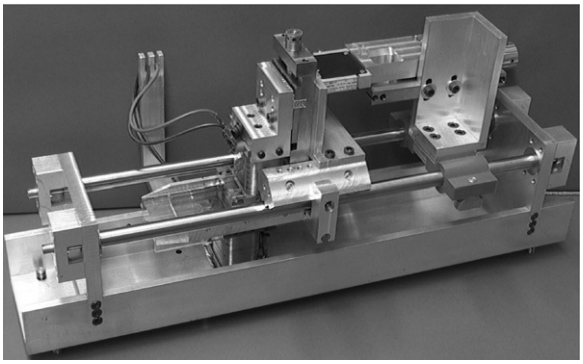

Figure 11. Photograph of the ferrofluid supported linear machine equipped for measuring lateral forces.

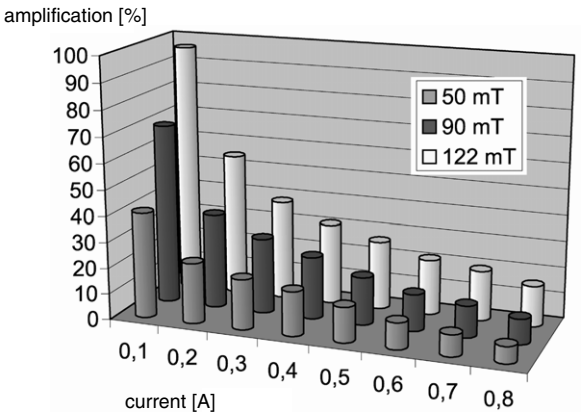

Figure 12. Enhancement of force by using three different ferrofluids (50 mT, 90 mT, 122 mT) with a gap width of 0.5 mm versus the coil current (3D columns).

- reproducible adjustability of the upper electromagnet to minimize the measuring error of force and nevertheless keeping a constant width of the gap between the two magnets;
- reliable enclosure of the ferrofluid between the magnetic poles.

In figure 12 the enhancement of force is presented for three different ferrofluids versus the coil current, which means the strength of the magnetic field in the gap. The gap width of 0.5 mm represents an average of applied electric motors.

In figure 13 are given exemplarily the force amplifications of all investigated ferrofluids (50 mT, 76 mT, 85 mT, 90 mT, 105.5 mT, 113 mT, 122 mT) with a gap width of 0.5 mm.

It can be recognized how the impact of the ferrofluids varies. Three fluids which differ from the trend are the following: these with 85 and 113 mT show a reduced magnification effect with the highest viscosity. The 76 mT fluid shows a strong effect despite the quite small saturation polarization.

Each of the investigated fluids is a laboratory made unique specimen. From this result the very different properties and effects.

In figure 14 the measurement of the lateral forces for the grooved magnet cores as a simulation for a stepping motor can be seen. The solid and dashed curves respectively are

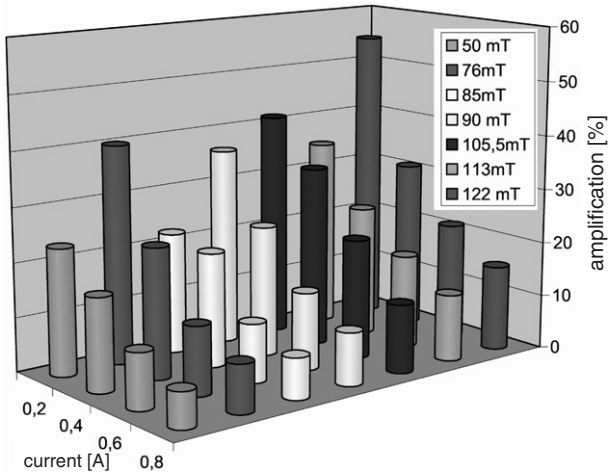

Figure 13. Enhancement of force for all analysed ferrofluids with a gap width of 0.5 mm versus the coil current (3D columns).

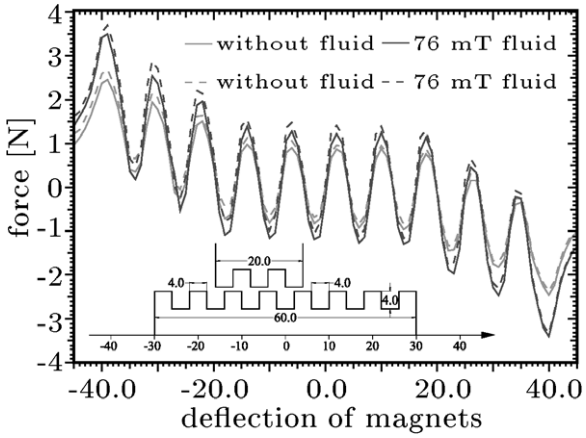

Figure 14. Lateral force versus the lateral deflection measured with the linear stepping motor simulator for a gap width of 1.5 mm.

two different measurement runs moving the upper magnet in the opposite direction. The light grey curves are taken without a fluid, the black ones with a 76 mT saturation magnetization ferrofluid. The intensification of the force for each step is evident. This intensifies the retention force, which is an important parameter for stepping motors. The difference of the forces by moving in opposite directions is due to properties of the experimental set-up.

3.2. Rotating electric machines

The 3D graph in figure 15 shows the structure of the modified asynchron machine. The interior is changed in such a way that the ferrofluid is held only in the gap between rotor and stator, other cavities are filled to reduce the amount of needed fluid, and the whole machine is sealed against leakage. It has to be taken into account that by filling the cavities the thermal conductance is reduced due to a lower heat transport caused by moving air. For an industrial prototype this has to be taken into account in order to take advantage of a higher heat transfer of the liquid

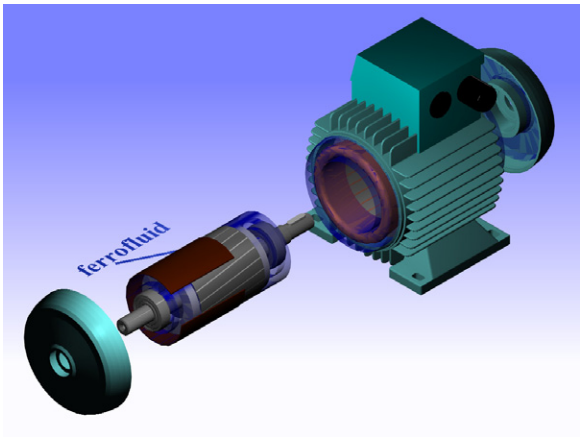

Figure 15. 3D presentation of the ferrofluid filled construction of the rotating asynchron electric machine.

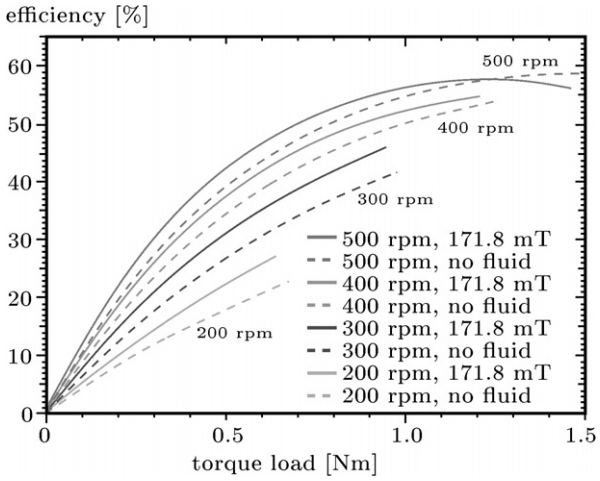

Figure 16. Efficiency of the induction motor for three different rotational velocities and a petroleum based ferrofluid with 171.84 mT saturation polarization and without a ferrofluid respectively.

filled gap as discussed before. The sealing of the rotating axis is a further aspect which has to be improved. The grooves for the copper coils along the gap are smoothed with synthetic resin to avoid additional friction. The rotational speed of the motor is adjusted with a frequency converter. To measure the torque a defined load must be given to the motor. This has be done with an eddy current brake. The exact derivation of the formula for the torque produced by the brake can be found in [8]. The torque is measured with a commercial torque meter based on DMS technology. Because the measurement values are flawed due to variations of the apparatus, a spline function is applied on the measurement series. This method can be found in [9]. In general it has to be noticed that for lower values of rpm the maximum load delivered by the eddy current brake is smaller. This is because the maximum current load of the brake is limited and the braking action is weaker the lower the speed.

In figure 16 the efficiency of the modified induction motor is depicted versus the loaded momentum for three different rotational speeds and the 171.84 mT ferrofluid as well as without

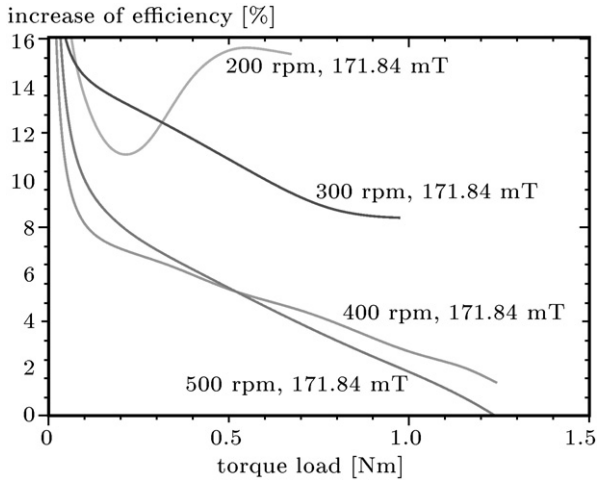

Figure 17. Increase of efficiency of the induction motor using four different rotational speeds with a kerosene based cobalt particle ferrofluid having a saturation polarization of 171.84 mT.

a ferrofluid for comparison. One can see an improvement of torque over the whole range of torque load. Only for very high loads is the effect lost. This may be due to measurement inaccuracies.

Figure 17 shows the increase of efficiency of the induction motor for the same data as before. Here the influence of the rotational speed is evident. For higher speeds the increase of efficiency is lower because of the greater friction.

3.3. Comparison with the calculations

The theoretical results are given in terms of forces for linear and torques for rotating machines. Figure 4 can be directly compared with figures 12 and 13 if one transfers the absolute values of figure 4 in relative amplification numbers with a value of about 30–40%. This corresponds very well with the measured figures taking into account the fluctuation margin of the measurements described in [5].

The efficiency from figure 16 is comparable with figure 7 by keeping in mind that the efficiency of an electric machine is related to the performance, which is directly proportional to the torque. The measured numbers are significantly lower compared with the theoretical results. This is not surprising because the friction of the rotation has to be added, apart from the fact that the modified induction machine used here is not perfectly suited for this operating mode.

4. Conclusion

The force amplification in electric machines using ferrofluids between the acting magnets has been proved theoretically and experimentally. The types of calculations presented here give a good impression of the effect of ferrofluids in the layer between stator and rotor and ensure the capacities for a further development resting on this technology. Especially in the case of rotating machines the combination of the segmentation of the volume filled with the ferrofluid on one hand and the recursive determination of the field dependent permeability on the other hand allows us to treat a nonlinear problem with a linear tool such as orthogonal expansion.

This theoretical result is a significant improvement of effectiveness for electric drives. The increased force is especially interesting for the holding moment in stepping motors, which is a crucial figure in their performance. Moreover, for traction engines the starting torque is an important parameter. Here the ferrofluid develops its capabilities, particularly since rotational friction, which lowers the force amplification, is totally absent here. Altogether the use of magnetic fluids in electric machines offers a wide variety of applications.

The treatment of thermal behaviour of the ferrofluid in the gap delivers a way to build more capable or compact electric machines.

The next step is to transfer this satisfying result to rotating machines. The results make it clear that a remarkable gain in effectiveness is achieved, but some additional difficulties occur here. For example, the technological question of safe enclosure of the fluid has to be solved. A ferrofluid based seal is an interesting option for this task.

References

[1] Boll R 1990 *Weichmagnetische Werkstoffe* (Vacuumschmelze GmbH, Siemens AG)
[2] Nethe A, Scholz Th and Stahlmann H 2004 Simulation of a ferrofluid-supported linear electric motor *Appl. Organometall. Chem.* 18
[3] Nethe A, Scholz Th and Stahlmann H 2004 *Increasing the ponderomotive interaction enforced by ferrofluids* Transworld Research Network, pp S351–82
[4] Engelmann S, Nethe A and Scholz Th 2004 Application of force enhancement with ferrofluids in a linear stepping motor model *J. Magn. Magn. Mater.* **270–276** S2345–7
[5] Engelmann S 2004 Aufbau eines rechnergestützten Messplatzes und Untersuchung der kraftverstärkenden Wirkung von Ferrofluiden im Luftspalt eines Linearmotors *Diplomarbeit at the BTU*
[6] Guyon E, Hulin J-P and Petit L 1997 *Hydrodynamik* (Vieweg Studium, Aufbaukurs Physik, Verlag Vieweg)
[7] Hoffmann H 1986 *Das Elektromagnetische Feld* (Berlin: Springer)
[8] Schieber D 2000 *Electromagnetic Induction Phenomena* (Berlin: Springer)
[9] Engeln-Müllges and Reutter F 1996 *Numerik-Algorithmen* VDI Verlag